IEEE Access
Multidisciplinary ⋮ Rapid Review ⋮ Open Access Journal

Received August 28, 2019, accepted September 10, 2019, date of publication September 13, 2019, date of current version October 1, 2019.

Digital Object Identifier 10.1109/ACCESS.2019.2941400

Hybrid Active Contours Driven by Edge and Region Fitting Energies Based on p-Laplace Equation

ASAD MUNIR[1], (Member, IEEE), SHAFIULLAH SOOMRO[2], (Member, IEEE), MUHAMMAD TANSEEF SHAHID[3], (Member, IEEE), TOUFIQUE AHMED SOOMRO[4], (Member, IEEE), AND KWANG NAM CHOI[3], (Member, IEEE)

[1]Department of Industrial and Information Engineering, Università degli Studi di Udine, 33100 Udine, Italy
[2]Quaid-e-Awam University of Engineering, Science and Technology, Campus Larkana, Larkana 77150, Pakistan
[3]Department of Computer Science and Engineering, Chung-Ang University, Seoul 156-756, South Korea
[4]School of Computing and Mathematics, Charles Sturt University, Sydney, NSW 2127, Australia

Corresponding author: Kwang Nam Choi (knchoi@cau.ac.kr)

This work was supported by the National Research Foundation of Korea (NRF) through the Korea Government (MSIT) under Grant 2019R1F1A1062612.

ABSTRACT By using local and global image information, a novel active contour method based on the p-Laplace equation for image segmentation is proposed in this paper. The force term in the evolution equation incorporates global, local and edge information of the image. The global and local terms drag the contour towards object boundaries precisely and take care of the contour movement when it is away from the object. Meanwhile, the integration of edge stopping function in this force term ensures the stoppage of contour at object boundaries to avoid boundary leakage problem. The variable exponent p-Laplace energy is used for smoothness of the level set to detect the exact object boundaries in the presence of complex topological changes and deep depression. Finally, the adaptive force and p-Laplace energy term are jointly integrated into a level set by using a simple finite difference scheme to build the final evolution equation for the method. The proposed method has strong capability to accurately segment the images having noise, intensity inhomogeneity, and complex object boundaries. Moreover, the proposed method overcomes the problem arise from contour initialization as the evolution of contour is independent of the initialization of level set function. Experimental results on synthetic, real and medical images along with two publicly available databases validate the robustness and effectiveness of the proposed method.

INDEX TERMS Level set, active contours, image segmentation, boundary detection.

I. INTRODUCTION

Boundary detection and image segmentation are very basic problems and have a significant effect in the fields of computer vision and image processing [1]. Image segmentation is a well-known technique which subdivides the image into particular regions to extract the meaningful objects from that image. The accuracy of this process is extremely effected when the image contains noise, low contrast, and intensity inhomogeneity. The occurrence of intensity inhomogeneity mostly depends on the spatial variations in illumination and defects in imaging devices which makes it difficult to isolate the object boundaries and background. Thus far, different techniques and approaches have been devised using the level set methods including active contour models in the field of image segmentation. In the beginning, Kass *et al.* [2] proposed an effective method for segmentation based on active contours which obtained closed and smooth boundaries, since then active contours have been frequently used in this area. The basic principle of active contours is deforming a curve towards object boundaries by using a force according to a partial differential equation [3]. These methodologies used several image characteristics like gradient, statistical and curvature information. Due to different image characteristics, the active contour models [4]–[29] are further divided into two categories: edge-based models [4]–[7], [20], [28] and region-based models [9]–[15], [15]–[19], [22]–[26], [29]. Edge-based models [4]–[7], [20], [28] use a balloon force

The associate editor coordinating the review of this manuscript and approving it for publication was Md. Asikuzzaman.

consist of image gradient information to drag the curve towards desired boundaries. These models are very strong in detecting distinct object boundaries but unable to segment the images having weak edges, intense noise, and blurred boundaries. On the contrary, Region-based models [9]–[19], [22]–[26], [29] perform accurately in the presence of fuzzy and weak boundaries as they use the information based on regions within the image.Classic region-based models consider the intensity of the whole image as homogeneous. Therefore, they fail to segment the images with intensity inhomogeneity. Both edge and region-based models have their own advantages and disadvantages. Edge-based models perform effectively when the objects in the image have a distinguished difference with the background and consist of sharp edges. On the other hand, region-based models can perform properly for the images having noise and weak boundaries as they use the statistical information of regions inside and outside the evolution curve. To obtain the benefits of both models we exploit edge and region-based information in the proposed method.

Region-based models are further classified into global [9], [10], [22], local [11]–[15] and hybrid [15]–[19], [23]–[26], [29] region based models. The most classical and famous global region based model is a Chan-Vese model [22] which is extracted from piecewise constant Mumford and Shah method [21]. This model works on the assumption that the given image has constant intensity values within the entire region. Therefore, the performance of this model is very poor for the images with intensity inhomogeneity. To resolve the problem of the previous model Li *et al.* proposed a local region based model known as LBF (local binary fitting) model [14]. This method utilize local image information and provide satisfactory results for the images having intensity inhomogeneity. Despite having a good performance for intensity inhomogeneity, this method is considerably sensitive to the initialization of the contour. Another local region based method called localized active contour method (LAC) [11] is proposed by Lankton and Tannenbaum. In this method global region-based methods are revised by substituting global region based information with image local information. This method performs well for intensity inhomogeneity and sensitive to the position of initial contour like other local region based models [11]–[15]. Due to the presence of local information terms in their formulations, these models also have high computational time complexity. Figure 1 shows the segmentation results of one inhomogeneous image. Figure 1(a) shows the result of the traditional Chan-Vese method while Figure 1(b) and Figure 1(c) display results of LBF and LAC methods respectively. It can be seen that local models handle intensity inhomogeneity properly unlike Chan-Vese model. To overcome the problem of contour initialization Wang and He [10] proposed a region based model in which contour can be initialized to any constant function. This method is totally independent of the position of initial contour but it fails to perform in the existence of intensity inhomogeneity. Zhou and Mu [28] introduced the p-Laplace equation in level set evolution to handle the complex topological changes and to precisely detect the boundary despite deep depression. Recently, Chenchung and Li [9] modified Bin Zhous work [28] by inserting Chan-Vese model with p-Laplace energy to form a level set equation. This model works accurately for the images having noise and blurred boundaries but unable to segment the inhomogeneous images. Previously, hybrid active contour models [16]–[19], [23]–[26], [29] have become very famous in solving these problems. These methods integrate region-based information with edge information to formulate an energy function. Due to the presence of both type of information they have higher accuracy when compared to the traditional edge or region based models. Oh *et al.* [17] has formulated a hybrid method by incorporating edge information into a region based energy function. This method uses the Chan-Vese model [22] and coupled it with geodesic edge term taken from GAC model [20] and accomplish results on medical images. Motivated by these previous works, we propose a novel adaptive active contour method in partial differential equation (PDE) formulation.

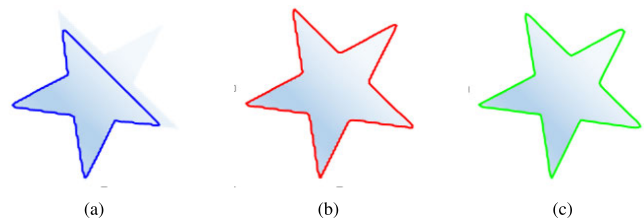

FIGURE 1. Segmentation of images having a white background and intensity inhomogeneity in objects a: Chan-Vese method. b: LBF method. c: LAC method.

In the proposed method, evolution equation is formed by a force, regularization and p-Laplace term. Force term consists of global, local and edge information. Global term drives the movement of the contour when it is away from the object while the local term controls the contour in the intensity varying area. The introduction of the scaled edge term ensures the stoppage of the contour at desired boundaries and overcomes the boundary leakage problem. The sign of this force term determines that the contour will move towards or away from the object boundary. The regulation term is responsible for controlling the smoothness of the level set function. The third term in the evolution equation is a p-Laplace energy term is also behaves as a regularization term. This p-Laplace term takes care of smoothness of the contour in the presence of noise [9]. Due to which, the proposed method is very effective in segmenting the noisy images along with the intensity inhomogeneity. The proposed approach completely eliminates the need for contour initialization as contour can be initialized to any bounded function (e.g. a constant function). By using the proposed method, experiments are conducted over several synthetic, real and medical images. Experiment results show that proposed scheme has a better performance than the previous techniques. Rest of this paper is structured as follows. In section 2, background and related previous methods are discussed. The proposed methodology is briefly explained in section 3. Experimental results and comparisons using synthetic and real images are shown in section 4. In the end, some conclusions are drawn in section 5.

II. BACKGROUND AND RELATED WORK

A. GEODESIC ACTIVE CONTOUR (GAC) METHOD

The GAC model [20] is a very basic active contour model for image segmentation which uses image gradient information to detect the boundaries of the objects in an image. In the given image $I : [0, a] \times [0, b] \rightarrow R^{+}$, let Ω be a bounded open subset of R^2 and $C(q) : [0, 1] \rightarrow R^2$ be a parameterized planer curve in this subset Ω. Then the GAC model is obtained by minimizing the following energy function:

$$E_{GAC}(C(q)) = \int_0^1 g(|\nabla I(C(q))|)C'(q)dq, \tag{1}$$

where g is the edge indicator function (ESF) given as follows:

$$g(\nabla I) = \frac{1}{1 + |\nabla G_\sigma * I|} \tag{2}$$

where G is a Gaussian kernel having standard deviation σ. By applying the calculation of variation [30], the Euler-Lagrange equation of Eq.(1) is as under:

$$C_t = g(|\nabla I|)\kappa \vec{N} - (\nabla g.\vec{N})\vec{N} \tag{3}$$

where N is the inward normal and κ denotes the curvature of the contour. To increase the speed of the propagation, a velocity term ? is added to the above equation and Eq.(3) can be rewritten as:

$$C_t = g(|\nabla I|)(\kappa + \alpha)\vec{N} - (\nabla g.\vec{N})\vec{N} \tag{4}$$

Then the final level set equation can be written as follows:

$$\frac{\partial \phi}{\partial t} = g(\nabla I)\left[div\left(\frac{\nabla \phi}{|\nabla \phi|}\right) + \alpha\right]|\nabla \phi| + \nabla g.\nabla \phi \tag{5}$$

where α denotes balloon force which is responsible for controlling the shrinking or expanding speed of the contour. This model uses the gradient information to detect the boundaries. Therefore, it fails in the presence of noise and blur boundaries.

B. THE CHAN-VESE (CV) MODEL

Chan-Vese [22] proposed an active contour model which is a special case of the most famous and basic region-based segmentation model, the Mumford-Shah model [21]. Let $I : \Omega \rightarrow R^2$ be an input image and C is a closed curve. Then the Chan-Vese model is expressed by the following energy function:

$$\begin{aligned} E_{CV}(C, c_1, c_2) = {} & \mu.length(C) + v.area(inside(C)) \\ & + \lambda_1 \int_{inside(C)} |I(x) - c_1|^2 H_\varepsilon(\phi(x))dx \\ & + \lambda_2 \int_{outside(C)} |I(x) - c_2|^2 (1 - H_\varepsilon(\phi(x)))dx \end{aligned} \tag{6}$$

where $\mu \geq 0$, $v \geq 0$, and $\lambda_1, \lambda_2 \geq 0$ are constants. The first and second terms in Eq.(6) are the Euclidean length of the closed curve C and area inside the closed curve C. $H_\varepsilon(\phi)$ is the regularized Heaviside function defined as:

$$H_\varepsilon(\phi) = \frac{1}{2}\left(1 + \frac{2}{\pi}\arctan\left(\frac{\phi}{\varepsilon}\right)\right) \tag{7}$$

where ε controls the smoothness of the Heaviside function. This model is based on the approximation of intensities values inside and outside the closed curve C which are defined as c_1 and c_2. Keeping ϕ fixed and minimizing energy function in Eq.(6), we have the values of c_1 and c_2 as follows:

$$c_1 = \frac{\int_\Omega I(x)H_\varepsilon(\phi(x))dx}{\int_\Omega H_\varepsilon(\phi(x))dx} \tag{8}$$

$$c_2 = \frac{\int_\Omega I(x)(1 - H_\varepsilon(\phi(x)))dx}{\int_\Omega (1 - H_\varepsilon(\phi(x)))dx} \tag{9}$$

By applying the gradient descent method [30], we obtain the following level set formulation:

$$\begin{aligned} \frac{\partial \phi}{\partial t} = \delta_\varepsilon(\phi)[\mu.div\left(\frac{\nabla \phi}{|\nabla \phi|}\right) - v - \lambda_1(I - c_1)^2 \\ - \lambda_2(I - c_2)^2)] \end{aligned} \tag{10}$$

where $\delta_\varepsilon(\phi)$ is the smooth version of Dirac delta function and is defined as:

$$\delta_\varepsilon(\phi) = \frac{\varepsilon}{\pi(\phi^2 + \varepsilon^2)} \tag{11}$$

Chan-Vese model [22] uses global characteristics of the image and considers intensity as homogeneous inside and outside the contour. Therefore, this method provides unsatisfied segmentation for the images having intensity inhomogeneity.

C. LOCALIZSED ACTIVE CONTOUR (LAC) MODEL

Lankton and Tannenbaum proposed a localized region-based active contour model [11] to express the inhomogeneity in images. The contour evolution is based on local region statistical information instead of global information. The basic idea of this model is to divide the inhomogeneous region into small homogeneous regions. For this purpose, this model uses a ball function which is defined as:

$$B(x, y) = \begin{cases} 1, & |x - y| < r \\ 0, & \text{otherwise} \end{cases} \tag{12}$$

where r denotes the radius and x is the center point of the ball function. When point y lies within the radius r of the ball function, this function is *1* and *0* otherwise. Using ball function $B(x, y)$, Lankton and Tannenbaum proposed the following energy function

$$E_{Local}(\phi, u_x, v_x) = \int_{\Omega_x} \delta_\varepsilon(\phi(x)) \int_{\Omega_y} B(x, y) .F(I(y), H(\phi(y)))dydx + \lambda \int_{\Omega_x} \delta_\varepsilon(\phi(x))\nabla\phi(x)dx \quad (13)$$

In the above equation(13)

$$F(I(y), H(\phi(y))) = H(\phi(y))(I(y) - u_x)^2 + (1 - H(\phi(y)))(I(y) - v_x)^2 \quad (14)$$

where u_x and v_x are the localized means inside and outside the contour respectively. These intensities are localized by ball function $B(x, y)$ at point x and are determined as:

$$u_x = \frac{\int_{\Omega_y} B(x, y)I(y)H_\varepsilon(\phi(y))dy}{\int_{\Omega_y} B(x, y)H_\varepsilon(\phi(y))dy} \quad (15)$$

$$v_x = \frac{\int_{\Omega_y} B(x, y)I(y)(1 - H_\varepsilon(\phi(y)))dy}{\int_{\Omega_y} B(x, y)(1 - H_\varepsilon(\phi(y)))dy} \quad (16)$$

By apply gradient descent method [30] and taking the first variation of Eq.(13) with respect to ϕ, the final level set equation is obtained as:

$$\frac{\partial\phi}{\partial t} = \delta_\varepsilon(\phi(x)) \int_{\Omega_y} B(x, y) \delta_\varepsilon(\phi(y))\Big((I(y) - u_x)^2 - (I(y) - v_x)^2\Big)dy + \lambda\delta_\varepsilon(\phi(x))div\left(\frac{\nabla\phi}{|\nabla\phi|}\right) \quad (17)$$

This method is capable of dealing images having intensity inhomogeneity and provides satisfactory segmentation results. The limitation of this model is that it is sensitive to the initial position of the contour.

D. WANG AND HE MODEL

To overcome the problem of contour initialization, Wang and He [10] proposed an adaptive level set evolution starting with a constant function. The evolution equation is consists of two forces: An adaptive force and a regularization force. Adaptive force is responsible for the movement of the contour and pulls the contour towards the object boundaries. Meanwhile, the regularization force controls the propagation speed and smoothness of the contour. The formulation of this approach is as follows:

$$\frac{\partial\phi}{\partial t} = \alpha F_{adp} + \beta F_{reg} \quad (18)$$

where α and β are the scaling constants. F_{adp} and F_{reg} are the adaptive and regularization forces respectively and are defined as:

$$F_{adp}(I, \phi) = g(|\nabla I|)sign\left(I(x, y) - \frac{c_1 + c_2}{2}\right) \quad (19)$$

$$F_{reg} = g(|\nabla I|)div\left(\frac{\nabla\phi}{|\nabla\phi|}\right) \quad (20)$$

In Eq.(19) and Eq.(20) g is the edge stopping function which stops the contour at desired boundaries and is given as:

$$g(|\nabla I|) = exp\left(-\frac{|\nabla I|}{20}\right) \quad (21)$$

The final form of this model in partial differential equation (PDE) framework on the level set function ϕ is defined as follows:

$$\frac{\partial\phi}{\partial t} = g(|\nabla I|)\left(\alpha f(I, c_1, c_2) + \beta div\left(\frac{\nabla\phi}{|\nabla\phi|}\right)\right) \quad (22)$$

where c_1 and c_2 are the intensities inside and outside the contour respectively. Adaptive force f is given as follow:

$$f(I, c_1, c_2) = sign\left(I(x, y) - \frac{c_1 + c_2}{2}\right) \quad (23)$$

This model [10] completely eliminates the need for initial contour as the level set can be initialized to any constant function. The limitation of this model is that it fails in segmenting the intensity inhomogeneous and too much noisy images.

E. ESRAC MODEL

Oh *et al.* [17] proposed a hybrid region and edge-based model named as edge scaled region-based active contour model by combining both edge and region-based information. This model integrated edge indicator function into Chan-Vese model and then scaled it with geodesic active contour model by using a weighted coefficient. This method has the following formulation.

$$E_{ESRAC} = \alpha\left(\int_\Omega g(I(x))|I(x) - c_1|^2dx + \int_\Omega g(I(x))|I(x) - c_2|^2dx\right) + (1 - \alpha)\int_0^L g\left(|\nabla I(C(q))|\right) ds \quad (24)$$

where α is a weighted parameter which is responsible for keeping a balance between region and geodesic edge term and its value is between $0 \leq \alpha \leq 1$. $g(x)$ is monotonically decreasing edge indicator function and is defined as:

$$g(I(x, y)) = \left(1 - \lambda\left|\nabla G_\sigma * I(x, y)\right|_\infty^2\right)_+^2 \quad (25)$$

Minimizing Eq.(24) by using gradient descent method [30], the final level set equation for this method is written as:

$$\frac{\partial\phi}{\partial t} = |\nabla\phi|\Big[\alpha\left(-g(I)(I - c_1)^2 + g(I)(I - c_2)^2\right) + (1 - \alpha)\Big(g(I)div\Big(\frac{\nabla\phi}{|\nabla\phi|}\Big) + \nabla g(I)\frac{\nabla\phi}{|\nabla\phi|} - v\Big)\Big] \quad (26)$$

By using edge and region information jointly, this method can segment blurred boundaries accurately. However, this method provides unacceptable results in the presence of intensity inhomogeneity.

F. P-LAPLACE EQUATION

Using the formulation of p-Laplace equation, Zhou and Mu [28] proposed a weighted p-Dirichlet integral as the geometric regularization on the zero level set for boundary extraction. The formulation of energy function is as follows:

$$E(\phi) = \lambda_d E_d(\phi) + \lambda_c E_c(\phi) + \lambda_p E_p(\phi) \tag{27}$$

where λ_d, λ_c, and λ_p are scaling constants.

$$E_d(\phi) = \frac{1}{2}\int_{\Omega} (|\nabla\phi - 1|)^2 \, d\Omega \tag{28}$$

$$E_c(\phi) = \int_{\Omega_c} |\nabla\phi|^2 d\Omega_c = \int_{\Omega} H(-\phi)|\nabla\phi|^2 d\Omega \tag{29}$$

$$E_p(\phi) = \int_{\Omega} \delta(\phi)|\nabla\phi|^p d\Omega \tag{30}$$

E_d is the energy used to keep the level set function close to signed distance function [7]. Energy E_c is used to drive the curve towards object boundaries and E_p is the weighted p-Dirichlet integral used to keep the contour smooth. The final evolution equation for this method is:

$$\frac{\partial\phi}{\partial t} = \lambda_d\left[\Delta\phi - div\left(\frac{\nabla\phi}{|\nabla\phi|}\right)\right] + \lambda_p\delta(\phi)div\left(g|\nabla\phi|^{p-2}\nabla\phi\right) + \lambda_c g\left[\delta(\phi)|\nabla\phi|^2 + 2div\left[H(-\phi)\nabla\phi\right]\right] \tag{31}$$

where g, $H(\phi)$, and $\delta(\phi)$ are the edge indicator, Heaviside and Dirac delta functions defined in Eq.(2), (7), and (11) respectively. Chencheng and Li [9] modified the above model by integrating degraded Chan-Vese model [18] into the previous model. The degraded Chan-Vese energy is defined as:

$$E_{DCV}(\phi) = \int_{\Omega}\left(I - \frac{c_1 + c_2}{2}\right)H(\phi)dx \tag{32}$$

where c_1 and c_2 are the intensities inside and outside the contour respectively and are defined in Eq.(8) and (9). The final level set Equation for this model is expressed as:

$$\frac{\partial\phi}{\partial t} = \delta(\phi)\left\{\alpha\left[\left(I - \frac{c_1 + c_2}{2}\right)\beta div\left(g|\nabla\phi|^{p(I_{LRS})-2}\nabla\phi\right)\right]\right\} \tag{33}$$

where $p(I_{LRS})$ is a value between $1 \le p(I_{LRS}) \le 2$ and is determined by image information. This method can deal well with the noisy images but fails to detect boundaries in the presence of intensity inhomogeneity.

III. ACTIVE CONTOURS DRIVEN BY LOCAL AND GLOBAL FITTING ENERGIES BASED ON P-LAPLACE EQUATION

In this section, we present a novel hybrid active contour model formed by using global and local region information along with scaled edge term and its formulation. The proposed method introduces a new force term by using the global and local region information integrated with gradient information. Global and local intensity information in the proposed force term drags the contour towards the object boundaries even in the presence of intensity inhomogeneity. While the gradient based edge term stops the contour at desired edges and avoids the boundary leakage problem. During the evolution of level set equation, the contour proceeds inward or outward due to the sign of the proposed force. Finally, a p-Laplace force is used in an additive way for the smoothness of the contour in the case of noisy images. Let $I : \Omega \subset R^2 \rightarrow R$ be the given image, then inspired by Wang and He model the level set equation of the presented method is given as follow:

$$\frac{\partial\phi}{\partial t} = \alpha F_{AGL} + \beta F_{PL} + \mu F_{REG} \tag{34}$$

where $\alpha, \beta, \mu > 0$ are constants and F_{AGL} in eq.(34) is the proposed adaptive global and local force term. We formed the global term by integrated edge information with Chan-Vese energy [22] which is given as:

$$E_{GE} = \int_{\Omega} g(\nabla I)\left|I(x) - c_1\right|^2 H(\phi(x))dx + \int_{\Omega} g(\nabla I)\left|I(x) - c_2\right|^2 (1 - H(\phi(x)))dx \tag{35}$$

E_{GE} is the global energy term in the proposed method. $g(\nabla I)$ is positive decreasing edge indicator function [17] and is defined in Eq.(2). c_1 and c_2 are the intensities inside and outside the contour and are expressed as:

$$c_1 = \frac{\int\limits_{\Omega} I(x)g(\nabla I)H_\varepsilon(\phi(x))dx}{\int\limits_{\Omega} g(\nabla I)H_\varepsilon(\phi(x))dx} \tag{36}$$

$$c_2 = \frac{\int\limits_{\Omega} I(x)g(\nabla I)(1 - H_\varepsilon(\phi(x)))dx}{\int\limits_{\Omega} g(\nabla I)(1 - H_\varepsilon(\phi(x)))dx} \tag{37}$$

The level set equation for global energy is [17]

$$\frac{\partial\phi}{\partial t} = \left|\nabla\phi\right|\left[-g(I)(I - c_1)^2 + g(I)(I - c_2)^2\right] \tag{38}$$

In the proposed method the local energy is formulated by coupling the edge function with localized active contour (LAC) method [11]. This local energy E_{LE} is defined as:

$$E_{LE} = \int_{\Omega} g(\nabla I)B(x,y)\left|I(x) - u\right|^2 H(\phi(x))dx + \int_{\Omega} g(\nabla I)B(x,y)\left|I(x) - v\right|^2 (1 - H(\phi(x)))dx \tag{39}$$

where $B(x, y)$ is a ball function defined in Eq.(12). u and v are the localized means inside and outside the contour and are redefined as:

$$u = \frac{\int_{\Omega_y} B(x,y)g(\nabla I)I(y)H_\varepsilon(\phi(y))dy}{\int_{\Omega_y} B(x,y)g(\nabla I)H_\varepsilon(\phi(y))dy} \tag{40}$$

$$v = \frac{\int_{\Omega_y} B(x,y)g(\nabla I)I(y)(1 - H_\varepsilon(\phi(y)))dy}{\int_{\Omega_y} B(x,y)g(\nabla I)(1 - H_\varepsilon(\phi(y)))dy} \tag{41}$$

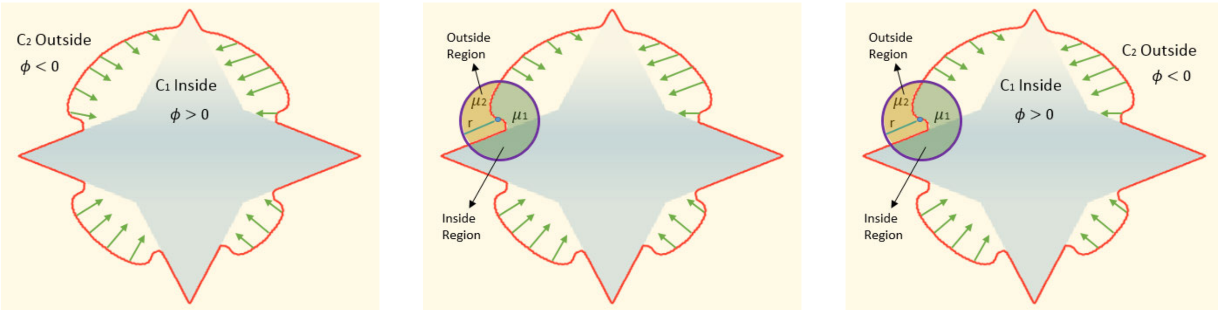

(a) (b) (c)

FIGURE 2. Graphical representation of the Adaptive global and local force. c_1 and c_2 are the global and μ_1 and μ_2 are the local intensity means (a) Global force coupled with edge function (b) Local force coupled with edge function (c) Combination of global, local and edge function.

By using gradient descent method [30] the level set equation for Eq.(39) is written as:

$$\frac{\partial \phi}{\partial t} = \left|\nabla \phi\right| \delta(\phi) \left[- g(I)B(x,y)(I-u)^2 + g(I)B(x,y)(I-v)^2 \right] \tag{42}$$

By using the Eq.(38) and Eq.(42) and applying the degraded Chan-Vese model [18], we proposed the following adaptive global and local force

$$F_{AGL} = sign\left(\left|\nabla \phi\right| g(\nabla I) \left(I - (w)\frac{c_1+c_2}{2} - (1-w)\frac{u+v}{2} \right) \right) \tag{43}$$

where w is the weight coefficient having values between *0* and *1*. Global and local intensities c_1, c_2, u and v are defined in Eq.(36), (37), (40) and (41). The movement of the contour during evolution process is monitored by this force as it changes its direction on the basis of the sign of the proposed adaptive force. If $F_{AGL}(x, y, \phi) < 0$, then $\frac{\partial \phi}{\partial t} < 0$, the level set function decreases and level set increases when F_{AGL} has a positive sign. By this change in sign, the contour can move up or down adaptively by utilizing image statistical information. Therefore, the function can be initialized to any constant function which constructs the zero level curve automatically. So this approach completely eliminates the need for initial contour. The behavior of the proposed force term is explained in Figure 2. When the value of w is closer to *1* then global force is dominant and it considers the intensity information inside and outside the contour as shown in Figure 2(a). Figure 2(b) shows the dominance of the local force as intensity within the local circle is used. Figure 2(c) illustrates the combination of local and global terms and green arrows describe the presence of edge stopping function in the adaptive global and local force. The existence of this edge stopping function in the force term avoids the contour to escape boundaries. The second term in Eq.(34) is the p-Laplace force which plays important role in smoothing the contour particularly in noisy images. This term is extracted from the p-Laplace energy which is defined as:

$$E_p = \int_{\Omega} g(|\nabla I|)\delta(\phi)\left|\nabla \phi\right|^p dx \tag{44}$$

where p is a parameter and its value varies between *1* to *2*. The p-Laplace force F_{PL} is derived from the Eq.(44) by taking its derivative with respect to ϕ. Finally, the p-Laplace force is given as follows:

$$F_{PL} = div\left(g(|\nabla I|)\left|\nabla \phi\right|^{p-2} \nabla \phi \right) \tag{45}$$

Third and last term in Eq.(34) is called the regularization term which is responsible for the smoothness of the zero level set and controls the occurrence of infrequent small contours in the final segmentation. This term can be written as:

$$F_{REG} = \Delta \phi \tag{46}$$

$$\Delta \phi = \frac{\partial^2 \phi}{\partial x^2} + \frac{\partial^2 \phi}{\partial y^2} \tag{47}$$

In this paper, we used Heaviside $H(\phi)$ and Delta Dirac $\delta(\phi)$ function as defined in Eq.(7) and Eq.(11). By combining all the three forces in Eq.(43), (45) and (46) the final level set equation for the proposed method is defined as:

$$\frac{\partial \phi}{\partial t} = \alpha sign \left(\left|\nabla \phi\right| g(\nabla I) \left(I - (w)\frac{c_1+c_2}{2} - (1-w)\frac{u+v}{2} \right) \right) + \beta div\left(g(|\nabla I|)\left|\nabla \phi\right|^{p-2} \nabla \phi \right) + \mu \Delta \phi \tag{48}$$

where $\alpha, \beta > 0$ are constant. As α gives weight to the force term so it is responsible for controlling the propagation speed of the level set function and β is used to detect the distinct or jagged boundaries. One more advantage of the proposed method is that it is independent of the position of initial contour. Therefore, the level set function is initialized to any constant function. The initialization of the contour for the proposed method is defined as:

$$\phi_0(x, y) = \rho, \quad (x, y) \in \Omega \tag{49}$$

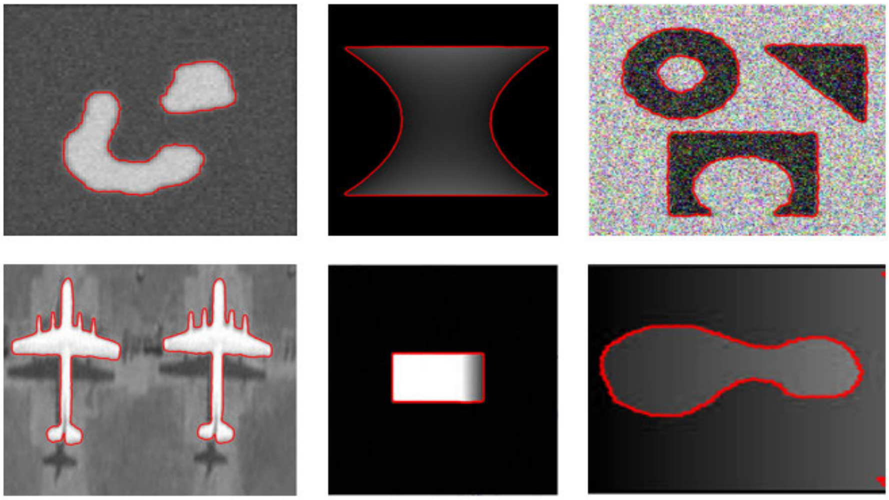

FIGURE 3. Results of the proposed method on different images.

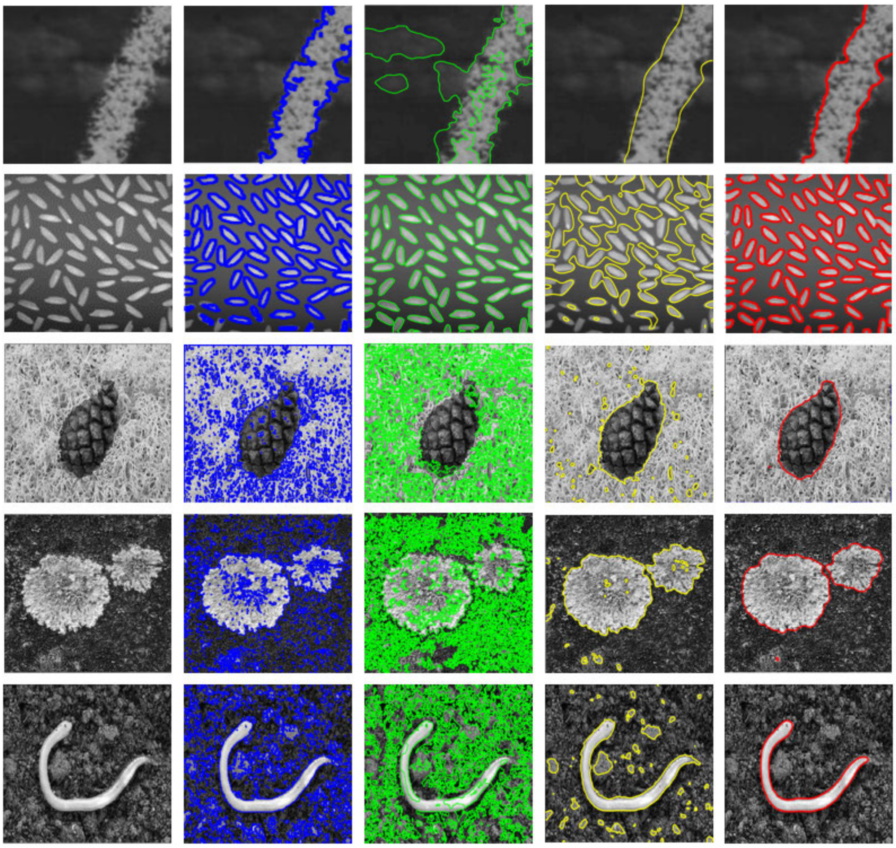

FIGURE 4. Segmentation results of four models for real images. The first column: Original images; the second to the fifth column: Segmentation results of Chan-Vese, LAC, Huang and the proposed method respectively with w = 0.001,0.001,0.002,0.001 and 0.002.

where ρ is a positive constant. In summary, the iterative steps of the suggested algorithm are given as follows:

IV. EXPERIMENTAL RESULTS AND DISCUSSION

In this section, the performance of the proposed method is elaborated on some synthetic, real and medical images. The results on all these images illustrate the robustness of the proposed method in comparison with the other methods. The proposed method is tested on various real and medical images selected from different repositories. This method is implemented and tested on MATLAB R2015a version installed in the 64-bit operating system (windows 7) having 3.40 GHz Intel Core-i7 microprocessor with 8 GB of RAM. There is no need of contour initialization in the proposed method, therefore, the initial level set function is initialized to a constant function, i.e. $\phi_0 = 2$ in all the experiments.

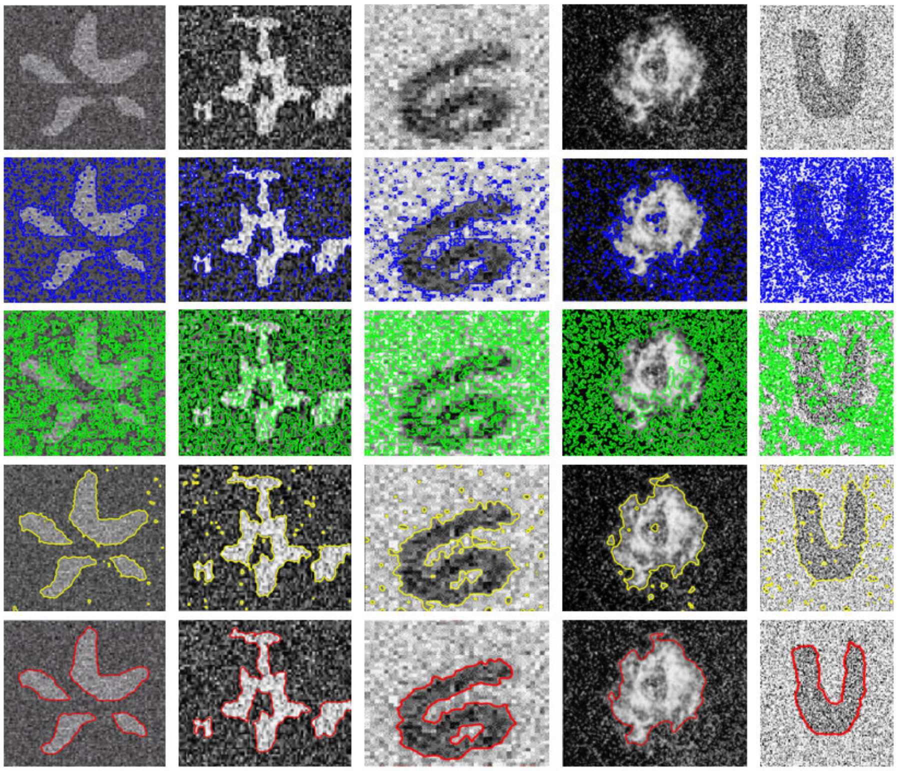

FIGURE 5. Segmentation results of four models for noisy images: (top row) original images; (second row) results of Chan-Vese model; (third row) results of LAC model; (fourth row) results of Huang model; (bottom row) results of the proposed model with w = 0.1, 0.3, 0.1, 0.4 and 0.2.

Algorithm

1) **Initialize** $\phi = \phi_0(x, y)$ with Eq (49)
2) $n = 1$.
3) **while** $n < N_{max}$ ***do***
4) Compute (2), (36), (37), (40) and (41) respectively.
5) Calculate forces by computing (43), (45),(46) respectively.
6) Evaluate ϕ using (48).
7) $n = n + 1$.
8) **end while**
9) **Output:** Final segmentation result, final ϕ.

The parameters used in all our experiments are $\alpha = 1$, $\beta = 1$, $\Delta t = 2$, $\mu = 0.003$, and $p = 1.99$. w is a weight variable so its value is different for every image $0 \leq w \leq 1$.We compared our results with CV model [22], LAC model [11], and Huang model [9] to verify the correctness of our method. We have tested our method on different categories of images as shown in Figure 3.The first image in the first row is a simple synthetic image while the second image does not have distinct boundaries. The third image in the top row shows the result of the proposed method on a noisy image. The second row in Figure 3 consists of an image having intensity variation in the background, an image contained inhomogeneous intensity object and an inhomogeneous image. The results on all categories of images show that the proposed method gives satisfactory performance on all these images. In Figure 4, results on some real images and comparison with other methods have shown. The images in the first and second row have small intensity changes at the edges of the objects. The last three rows have the images with complex background therefore in all other methods the contour is completely failed to detect the boundaries. The proposed method is segmenting all these objects precisely even in the presence of complex background.

Figure 5 explains the comparison of the proposed method with other three models for segmentation of some noisy images. The first row consists of original images while the next three rows show the results for Chan and Vese [22], LAC [11] and Huang model [9] respectively. The results of the proposed method are shown in the last row in Figure 5. In the results of CV and LAC models, the contour is scattered in all the images and fail to distinguish object boundaries from the background. Huang model provides some good results in comparison to the other methods but fails to give smooth contour at the object boundaries. The results of the proposed method prove that this technique can easily overcome the presence of noise in the images. The results of the proposed method on some inhomogeneous images and their comparison with other methods are displayed in Figure 6. CV [22] and Huang [9] models

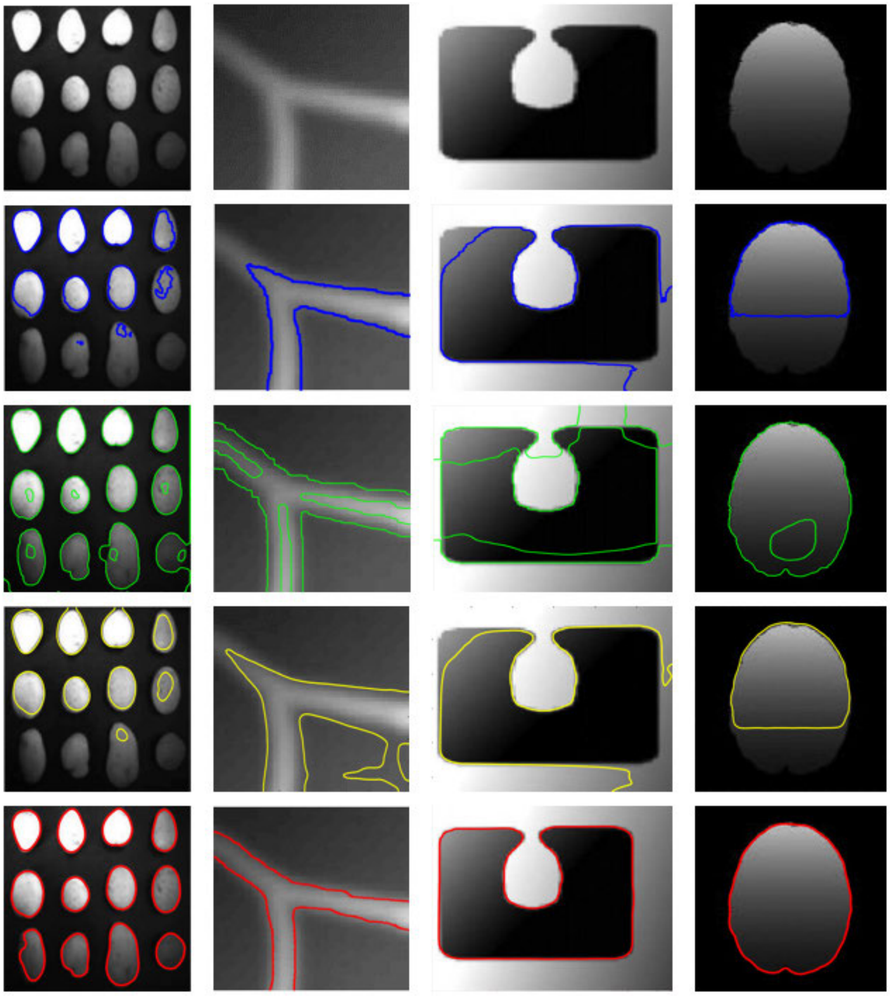

FIGURE 6. Segmentation results of four models on some synthetic images: (top row) original images; (second row) results of Chan-Vese model; (third row) results of LAC model; (fourth row) results of Huang model; (bottom row) results of the proposed model with w = 0.001, 0.001, 0.002, 0.001 and 0.003.

completely fail to segment the objects when the images have inhomogeneous intensity because these model only use the global image information. LAC model [11] is a local model but the results of this model are not satisfactory as it is much sensitive to the position of initial contour. The performance of the proposed method on inhomogeneous images is more acceptable as compared to all other three methods.

The results of the proposed method on some inhomogeneous images and their comparison with other methods are displayed in Figure 6. CV [22] and Huang [9] models completely fail to segment the objects when the images have inhomogeneous intensity because these model only use the global image information. LAC model [11] is a local model but the results of this model are not satisfactory as it is much sensitive to the position of initial contour. The performance of the proposed method on inhomogeneous images is more acceptable as compared to all other three methods.

Figure 7 illustrates the results of the proposed and other three methods on the real images taken from Caltech database [34]. All these images are selected from different categories of that database. The first image is taken from brain category while second, third and fourth are selected from tick, starfish and airplane category respectively. The first column in Figure 7 contained original images with their ground truths and second, third and fourth columns show the results for CV [22], LAC [11], and Huang [9] method respectively. As shown in Figure 7 the results of all the other three methods are not accurate as compared to their ground truths. The last column has the segmentation results of the proposed method and these results are exactly matching with the respective ground truths. So the proposed method performs well on the real images as well in comparison to the other three methods. The proposed method provides satisfactory results on many synthetic and real images. This method also overcome the problem of contour initialization and eliminates the need for

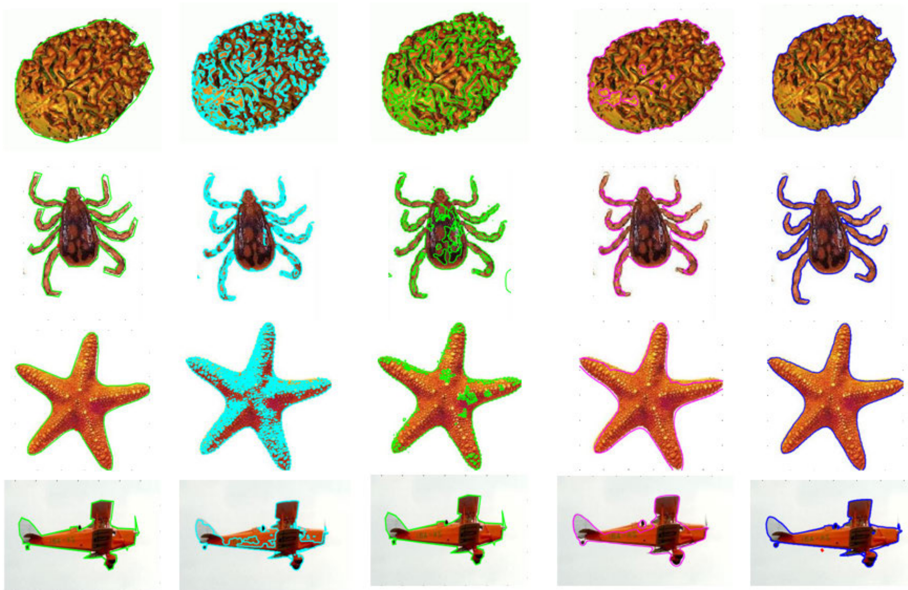

FIGURE 7. Segmentation results of four models for real images from Caltech database. The first column: Original images with ground truth; second column: Results of Chan-Vese; third column: Results of LAC; second column: Results of Huang and last column: Segmentation results of the proposed method.

initial contour. So the level set function can be initialized to any constant function and we used $\phi_0 = 2$ in all these experiments.

V. QUANTITATIVE ANALYSIS

This section explains the quantitative analysis of the results of the proposed method and compared them with other state-of-the-art methods.

A. EVOLUTION ON SKIN LESION IMAGES (PH^2 DATABASE)

In the recent years, the pace of skin cancer has been increasing consciously and Melanoma is its dead-dealing form [31]. Early detection and proper treatment play a critical role to increase the rate of survivals. Many researchers worked to detect melanoma in skin lesion images in these past years. Therefore, we applied the proposed method on a publically available database named as PH^2 database [33]. Figure 8 shows the results on images taken from that database and the proposed method performance is quite acceptable when compared with the ground truths. The green color contour is the ground truth and the magenta color contour is the result of the proposed method on dermoscopic images. In Table 1, we compared the proposed method on PH^2 database [33] to verify the performance of this method over the other three methods. Accuracy term tells us the overall accuracy of the segmentation result across the whole image domain. For accuracy calculations, the sum of all the true positives (TP) and true negatives (TN) is divided by the sum of true positives, true negatives, false positives (FP) and false negatives (FN) as given in Eq. (50). Moreover, we have also computed and compared the CPU time and iterations of each method in Table 2. It shows that, proposed method is also efficient in terms of time accompanied with previous methods.

TABLE 1. Comparison of the proposed method with traditional methods over PH^2 database [33].

Methods	Specificity	Sensitivity	Accuracy
Chan-Vese [22]	91.5	90.2	87.6
LAC [11]	83.5	88.6	87.1
Huang [9]	94.9	94.1	92.4
Zhang et al [32]	92.5	93.6	95.7
Proposed	97.3	94.6	96.7

TABLE 2. Average CPU time(in seconds) and iterations consumed by each method over PH^2 database [33].

Methods		
Chan-Vese [22]	Iterations	20
	CPU time(sec)	4.652
LAC [11]	Iterations	50
	CPU time(sec)	12.568
Huang [9]	Iterations	40
	CPU time(sec)	17.265
Zhang et al [32]	Iterations	32
	CPU time(sec)	10.256
Proposed method	Iterations	15
	CPU time(sec)	5.773

$$Accuracy = \frac{(TN + TP)}{(TP + FP + TN + FN)} \tag{50}$$

Specificity shows the ignorance of the true negative region during segmentation while the sensitivity describes that

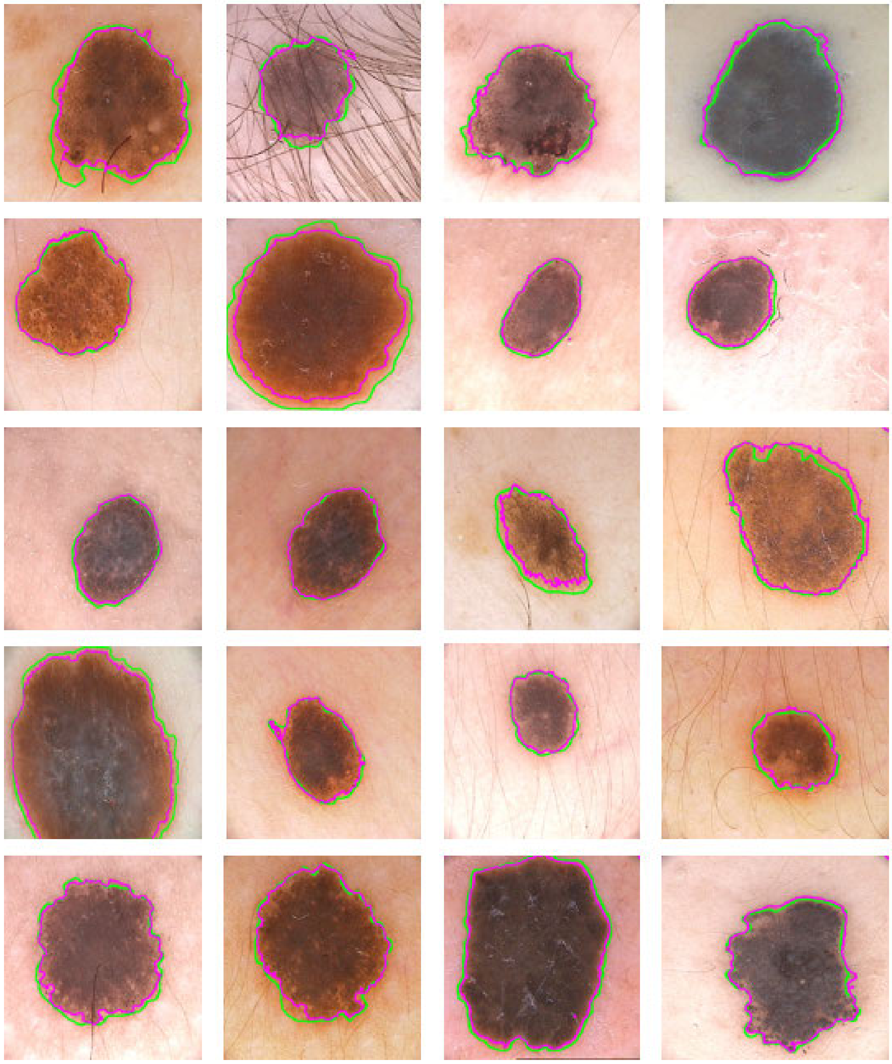

FIGURE 8. Segmentation results of the proposed model on dermoscopic images are taken from PH^2 database [33]: Green contour represents the ground truth and magenta contour shows the Results of the proposed model.

whether obtained information has same information we need without considering false positives. The specificity and sensitivity are calculated as follows:

$$Specificity = \frac{(TN)}{(TN + FP)} \tag{51}$$

$$Sensitivity = \frac{(TP)}{(TP + FN)} \tag{52}$$

Table 1 describes that the proposed method has better results in terms of specifity, senstivity and accuracy among all these methods and is capable of detecting melanoma in many skin lesion images correctly.

B. EVOLUTION ON REAL IMAGES (CALTECH DATABASE)

To validate our method on real images, we selected another publically available database known as Caltech database [34]. This database has different categories of objects contained many real images. We applied our method on some images from several categories to prove the correctness of the method. Figure 9 shows the segmentation results of the proposed method along with the ground truths. The first row consists of the images from categories anchor, brain, airplanes, and starfish. The blue and yellow contours are ground truths while green and red contours are the results of the proposed method for all the images in Figure 9. In the second row, images are selected from bonsai, brontosaurus, lotus, and dragonfly from left to right respectively. The third row contained images from flamingo, tick, wrench, and umbrella while the last row has images from menorah, butterfly, bonsai and lotus categories from left to right respectively. Figure 9 shows that in every image the resulting contour of the proposed method overlaps the ground truths. Figure 10 explains the quantitative analysis of the proposed method on the real

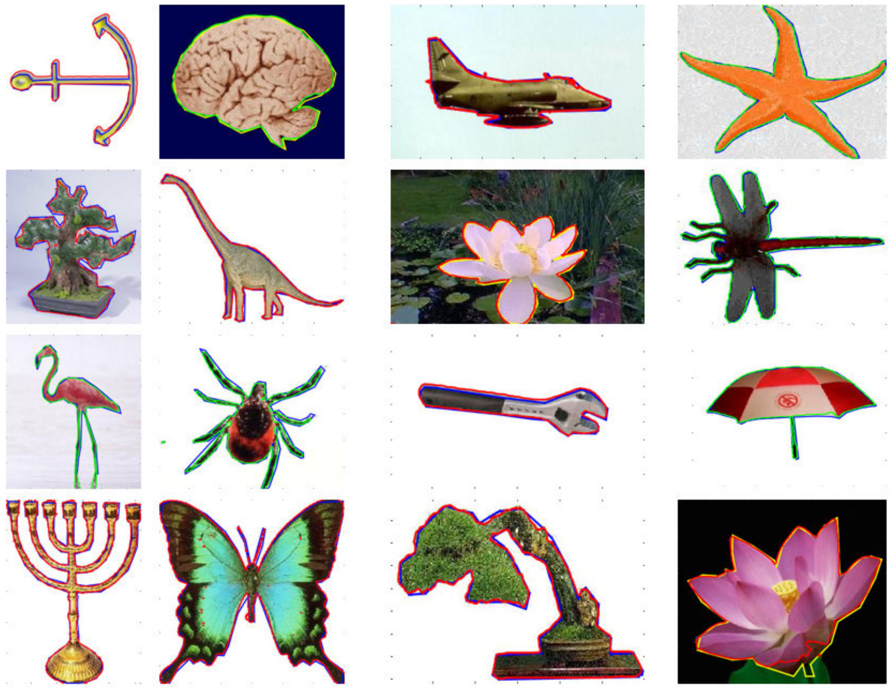

FIGURE 9. Segmentation results of the proposed model on real images taken from Caltech database [34]: Blue and yellow are the ground truths while red and green contours show the results of the proposed model.

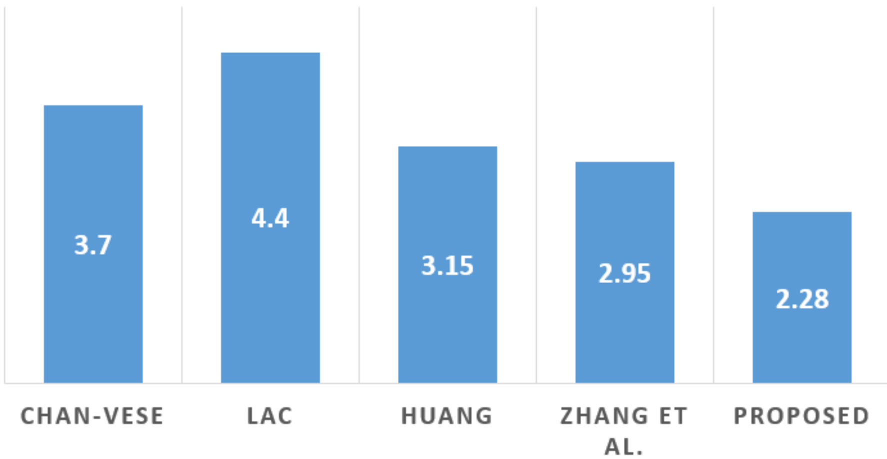

FIGURE 10. Hausdorff distance comparison of the proposed method with different methods for real images from Caltech database.

images collected from Caltech database. For comparison with the other method, we calculate Hausdorff distance (HD) for all the methods. HD is the measurement of the distance between the ground truth contour (GT) and the final segmented contour (FS). So for the good segmentation result HD should be minimum and Figure 10 shows our method has the minimum value of HD along with all these methods. For best segmentation results Hausdorff distance should be close to *0*. HD is calculated by the following equation. We have also computed and compared the Average CPU time and iterations of each method in Table 3. Results has out performed the previous methods in efficiency and time.

$$HD(GT, FS) = \max(\max_i\{d(gt_i, FS)\}, \max_j\{d(fs_j, GT)\}) \tag{53}$$

where GT and FS contours contain set of points $GT = \{gt_1, gt_2, gt_3, \ldots, gt_n\}$, $FS = \{fs_1, fs_2, fs_3, \ldots, fs_n\}$ respectively, and d is the distance from gt_i to the closest point on contour FS. Segmentation results show that the proposed method has satisfactory performance on real images as well.

TABLE 3. Average CPU time (in seconds) and iterations consumed by each method over Caltech database [34].

Methods		
Chan-Vese [22]	Iterations CPU time(sec)	25 6.654
LAC [11]	Iterations CPU time(sec)	100 25.584
Huang [9]	Iterations CPU time(sec)	50 22.965
Zhang et al [32]	Iterations CPU time(sec)	36 11.875
Proposed method	Iterations CPU time(sec)	20 8.324

VI. CONCLUSION

This paper presents a hybrid region-based active contour model for image segmentation by using (PDE) formulation. The evolution of contour is controlled by a force term, p-Laplace term, and a regularization term. To achieve the accurate results and enhance the performance of the method, we coupled edge indicator function into global and local intensity information to formulate an adaptive force. Due to the use of both intensity information and integration of the edge stopping function in adaptive force, the proposed method provides accurate segmentation results on various types of images. The edge stopping function is used to stop the contour at the required boundaries and to avoid boundary leakage problem. The p-Laplace force is used to keep the evolution of contour smooth for noisy images. Moreover, the need of initial contour is completely eliminated as the level set function can be initialized to any constant function. A simple explicit finite difference scheme having a larger time step is used to implement the given algorithm. This method is able to segment the noisy and inhomogeneous images properly. Experimental results prove that the proposed algorithm yields better segmentation results for many synthetic, real and medical images. Furthermore, comparison results with the other methods and evaluation on PH^2 and Caltech datebases verify the robustness of our technique.

CONFLICT OF INTERESTS

The authors declare that there is no conflict of interest regarding the publication of this article.

REFERENCES

[1] A. Elnakib, G. Gimel'farb, J. S. Suri, and A. El-Baz, "Medical image segmentation: A brief survey," in *Multi Modality State-of-the-Art Medical Image Segmentation and Registration Methodologies*. New York, NY, USA: Springer, 2011, pp. 1–39.

[2] M. Kass, A. Witkin, and D. Terzopoulos, "Snakes: Active contour models," *Int. J. Comput. Vis.*, vol. 1, no. 4, pp. 321–331, 1988.

[3] S. Osher and J. A. Sethian, "Fronts propagating with curvature-dependent speed: Algorithms based on Hamilton-Jacobi formulations," *J. Comput. Phys.*, vol. 79, no. 1, pp. 12–49, 1988.

[4] V. Caselles, F. Catté, T. Coll, and F. Dibos, "A geometric model for active contours in image processing," *Numerische Mathematik*, vol. 66, no. 1, pp. 1–31, 1993.

[5] R. Goldenberg, R. Kimmel, E. Rivlin, and M. Rudzsky, "Fast geodesic active contours," *IEEE Trans. Image Process.*, vol. 10, no. 10, pp. 1467–1475, Oct. 2001.

[6] C. Li, C. Xu, C. Gui, and M. D. Fox, "Distance regularized level set evolution and its application to image segmentation," *IEEE Trans. Image Process.*, vol. 19, no. 12, pp. 3243–3254, Dec. 2010.

[7] C. Li, C. Xu, C. Gui, and M. D. Fox, "Level set evolution without re-initialization: A new variational formulation," in *Proc. IEEE Comput. Soc. Conf. Comput. Vis. Pattern Recognit. (CVPR)*, vol. 1, Jun. 2005, pp. 430–436.

[8] S. Soomro, T. A. Soomro, and K. N. Choi, "An active contour model based on region based fitting terms driven by p-Laplace length regularization," *IEEE Access*, vol. 6, pp. 58272–58283, 2018.

[9] C. Huang and L. Zeng, "Level set evolution model for image segmentation based on variable exponent p-Laplace equation," *Appl. Math. Model.*, vol. 40, pp. 7739–7750, Sep. 2016.

[10] Y. Wang and C. He, "Adaptive level set evolution starting with a constant function," *Appl. Math. Model.*, vol. 36, pp. 3217–3228, Jul. 2012.

[11] S. Lankton and A. Tannenbaum, "Localizing region-based active contours," *IEEE Trans. Image Process.*, vol. 17, no. 11, pp. 2029–2039, Nov. 2008.

[12] L. Wang, Y. Chang, H. Wang, Z. Wu, J. Pu, and X. Yang, "An active contour model based on local fitted images for image segmentation," *Inf. Sci.*, vols. 418–419, pp. 61–73, Dec. 2017.

[13] J. Miao, T.-Z. Huang, X. Zhou, W. Xiaobing, Y. Wang, and J. Liu, "Image segmentation based on an active contour model of partial image restoration with local cosine fitting energy," *Inf. Sci.*, vol. 447, pp. 52–71, Jun. 2018.

[14] C. Li, C.-Y. Kao, J. C. Gore, and Z. Ding, "Minimization of region-scalable fitting energy for image segmentation," *IEEE Trans. Image Process.*, vol. 17, no. 10, pp. 1940–1949, Oct. 2008.

[15] K. Zhang, H. Song, and L. Zhang, "Active contours driven by local image fitting energy," *Pattern Recognit.*, vol. 43, no. 4, pp. 1199–1206, Apr. 2010.

[16] X. Jiang, B. Li, Q. Wang, and P. Chen, "A novel active contour model driven by local and global intensity fitting energies," *Optik*, vol. 125, pp. 6445–6449, Nov. 2014.

[17] J. Oh, D. R. Martin, and X. Hu, "Partitioned edge-function-scaled region-based active contour (p-ESRAC): Automated liver segmentation in multiphase contrast-enhanced MRI," *Med. Phys.*, vol. 41, Apr. 2014, Art. no. 041914.

[18] S. Liu and Y. Peng, "A local region-based Chan–Vese model for image segmentation," *Pattern Recognit.*, vol. 45, no. 7, pp. 2769–2779, Jul. 2012.

[19] H. Wang, T.-Z. Huang, Z. Xu, and Y. Wang, "An active contour model and its algorithms with local and global Gaussian distribution fitting energies," *Inf. Sci.*, vol. 263, pp. 43–59, Apr. 2014.

[20] V. Caselles, R. Kimmel, and G. Sapiro, "Geodesic active contours," *Int. J. Comput. Vis.*, vol. 22, no. 1, pp. 61–79, 1997.

[21] D. Mumford and J. Shah, "Optimal approximations by piecewise smooth functions and associated variational problems," *Commun. Pure Appl. Math.*, vol. 42, no. 5, pp. 577–685, 1989.

[22] T. F. Chan and L. A. Vese, "Active contours without edges," *IEEE Trans. Image Process.*, vol. 10, no. 2, pp. 266–277, Feb. 2001.

[23] S. Soomro, F. Akram, J. H. Kim, T. A. Soomro, and K. N. Choi, "Active contours using additive local and global intensity fitting models for intensity inhomogeneous image segmentation," *Comput. Math. Methods Med.*, vol. 2016, Sep. 2016, Art. no. 9675249.

[24] S. Soomro, A. Munir, and K. N. Choi, "Hybrid two-stage active contour method with region and edge information for intensity inhomogeneous image segmentation," *PLoS ONE*, vol. 13, no. 1, Jan. 2018, Art. no. e0191827.

[25] A. Munir, S. Soomro, C. H. Lee, and K. N. Choi, "Adaptive active contours based on variable kernel with constant initialisation," *IET Image Process.*, vol. 12, no. 7, pp. 1117–1123, 2018.

[26] S. Soomro, F. Akram, A. Munir, C. H. Lee, and K. N. Choi, "Segmentation of left and right ventricles in cardiac MRI using active contours," *Comput. Math. Methods Med.*, vol. 2017, Aug. 2017, Art. no. 8350680.

[27] L. Wang, L. He, A. Mishra, and C. Li, "Active contours driven by local Gaussian distribution fitting energy," *Signal Process.*, vol. 89, no. 12, pp. 2435–2447, Dec. 2009.

[28] B. Zhou and C.-L. Mu, "Level set evolution for boundary extraction based on a p-Laplace equation," *Appl. Math. Model.*, vol. 34, pp. 3910–3916, Dec. 2010.

[29] L. Wang, C. Li, Q. Sun, D. Xia, and C.-Y. Kao, "Active contours driven by local and global intensity fitting energy with application to brain MR image segmentation," *Comput. Med. Imag. Graph.*, vol. 33, no. 7, pp. 520–531, Oct. 2009.

[30] G. Aubert and P. Kornprobst, *Mathematical Problems in Image Processing: Partial Differential Equations and the Calculus of Variations*, vol. 147. Springer, 2006. [Online]. Available: https://books.google.com.pk/books?hl=en&lr=&id=MACXNooK-VIC&oi=fnd&pg=PR10&dq=G.+Aubert+and+P.+Kornprobst,+Mathematical+Problems+in+Image+Process734+ing:+Partial+Differential+Equations+and+the+Calculus+of+Variations,+vol.+147.+AQ:6+735+Springer,+2006&ots=dq5YNnUJ1U&sig=pZZt2KmJyhh7hG-i09QzjR–ELY&redir_esc=y#v=onepage&q&f=false

[31] T. Yao, Z. Wang, Z. Xie, J. Gao, and D. D. Feng, "A multiview joint sparse representation with discriminative dictionary for melanoma detection," in *Proc. Int. Conf. Digit. Image Comput., Techn. Appl. (DICTA)*, Nov./Dec. 2016, pp. 1–6.

[32] K. Zhang, L. Zhang, K.-M. Lam, and D. Zhang, "A level set approach to image segmentation with intensity inhomogeneity," *IEEE Trans. Cybern.*, vol. 46, no. 2, pp. 546–557, Feb. 2016.

[33] T. Mendon, P. M. Ferreira, J. S. Marques, A. R. S. Marcal, and J. Rozeira, "PH^2-a dermoscopic image database for research and benchmarking," in *Proc. 35th Annu. Int. Conf. IEEE Eng. Med. Biol. Soc. (EMBC)*, Jul. 2013, pp. 5437–5440.

[34] F.-F. Li, M. Andreetto, and M. Ranzato. (2018). *Caltech 101*. [Online]. Available: http://www.vision.caltech.edu/Image_Datasets/Caltech101/

ASAD MUNIR received the bachelor's degree in engineering sciences from GIK Institute, Pakistan, in 2013, and the master's degree in computer science from Chung-Ang University, South Korea, in 2018. He is currently pursuing the Ph.D. degree with the Department of Industrial and Information Engineering, Università degli Studi di Udine, Italy. His current research interests include object segmentation, object tracking, and person re-identification.

SHAFIULLAH SOOMRO received the B.E. degree from QUEST Nawabshah, Sindh, Pakistan, in 2008, the M.E. degree from MUET Jamshoro, Sindh, in 2014, and the Ph.D. degree in computer science from the Chung-Ang University, Seoul, South Korea, in 2018. He is currently an Assistant Professor in computer science with the Quaid-e-Awam University of Engineering, Science and Technology, Campus Larkana, Sindh. His current research interests include motion tracking, object segmentation, and 3D image recognition.

MUHAMMAD TANSEEF SHAHID received the bachelor's degree in engineering sciences from the GIK Institute, Pakistan, in 2014. He is currently pursuing the M.S. degree with the Department of Computer Science and Engineering, Chung-Ang University, Seoul, South Korea. His current research interests include object segmentation, object tracking, and person re-identification.

TOUFIQUE AHMED SOOMRO received the B.E. degree in electronic engineering from the Mehran University of Engineering and Science Technology, Pakistan, in 2008, and the M.Sc. degree in electrical and electronic engineering from the Universiti Teknologi PETRONAS, Malaysia, in 2014. He is currently pursuing the Ph.D. degree with the School of Computing and Mathematics, Charles Sturt University, Australia. His current research interests include most aspects of image enhancement and image analysis for medical images. He is currently implementing software-based algorithm for the detection of eye-related disease.

KWANG NAM CHOI received the B.S. and M.S. degrees from the Department of Computer Science, Chung-Ang University, Seoul, South Korea, in 1988 and 1990, respectively, and the Ph.D. degree in computer science from the University of York, U.K., in 2002. He is currently a Professor with the School of Computer Science and Engineering, Chung-Ang University. His current research interests include motion tracking, object categorization, and 3D image recognition.